Zeitschrift: Schweizerische mineralogische und petrographische Mitteilungen = Bulletin suisse de minéralogie et pétrographie

Band: 79 (1999)

Heft: 3

Artikel: The Dutung-Thaktote extensional fault zone and nappe structures documented by illite crystallinity and clay-mineral paragenesis in the Tethys Himalaya between Spiti river and Tso Morari, NW India

Autor: Girard, Matthieu / Steck, Albrecht / Thélin, Philippe

DOI: https://doi.org/10.5169/seals-60216

SCHWEIZ. MINERAL. PETROGR. MITT. 79, 419–430, 1999

The Dutung-Thaktote extensional fault zone and nappe structures documented by illite crystallinity and clay-mineral paragenesis in the Tethys Himalaya between Spiti river and Tso Morari, NW India

by *Matthieu Girard*[1], *Albrecht Steck*[1] and *Philippe Thélin*[1]

Abstract

Numerous measurements by XRD of the Scherrer width at half-peak height (001 reflection of illite), coupled with analyses of clay-size assemblages, provide evidence for strong variations in the conditions of low temperature metamorphism in the Tethyan Himalaya metasediments between the Spiti river and the Tso Morari.

Three sectors can be distinguished along the Spiti river-Tso Morari transect. In the SW, the Takling and Parang La area is characterised by a metamorphism around anchizone-epizone boundary conditions. Further north, in the Dutung area, the metamorphic grade abruptly decreases to weak diagenesis, with the presence of mixed-layered clay phases. At the end of the profile towards the NE, a progressive metamorphic increase up to greenschist facies is recorded, marked by the appearance of biotite and chloritoid.

The combination of these data with the structural observations permits to propose that a nappe stack has been crosscut by the younger Dutung-Thaktote extensional fault zone (DTFZ). The change in metamorphism across this zone helps to assess the displacements which occurred during synorogenic extension. In the SW and NE parts of the studied transect, a burial of 12 km has been estimated, assuming a geothermal gradient of 25 °C/km. In the SW part, this burial is due to the juxtaposition of the Shikar Beh and Mata nappes and in the NE part, solely to burial beneath the Mata nappe. In the central part of the profile, the effect of the DTFZ is to bring down diagenetic sediments in-between the two aforesaid metamorphic zones. The offset along the Dutung-Thaktote normal faults is estimated at 16 km.

Keywords: illite, Scherrer width, metamorphism, nappe tectonics, synorogenic extension, Tethyan Himalaya.

Résumé

De nombreuses mesures de la largeur de Scherrer à mi-hauteur du pic 001 de l'illite (FWHM, analysé par DRX), couplées avec l'analyse des paragenèses argileuses, ont permis de mettre en évidence un faible métamorphisme dans les métasédiments de l'Himalaya Tethysien, entre la rivière du Spiti et le Tso Morari.

Trois secteurs peuvent être distingués. Au SW, la région des cols (Takling et Parang La) est caractérisée par un métamorphisme à la limite anchizone-épizone. Plus au nord, dans la région de Dutung, le métamorphisme diminue brusquement pour atteindre le début de la diagenèse (présence de phases interstratifiées). L'extrémité NE du profil montre une augmentation progressive du métamorphisme jusque dans le faciès schiste vert, avec apparition de biotite et de chloritoïde.

La confrontation de ces données avec les observations structurales nous permet de mettre en évidence un empilement de nappes, recoupé par la zone de failles normales de Dutung-Thaktote (DTFZ). Les variations du métamorphisme le long du profil permettent d'estimer l'extension synorogénique. Dans les parties SW et NE du profil, un enfouissement de 12 km a pu être estimé en admettant un gradient géothermique de 25 °C/km. Cet enfouissement est dû, dans la partie SW, à la juxtaposition des nappes de Shikar Beh et du Mata et dans la partie NE, à la nappe du Mata uniquement. Dans la partie centrale du profil, la DTFZ permet de rabaisser des sédiments diagénétiques entre les deux zones anchi- à épizonales. Le rejet le long de la zone de failles de Dutung-Thaktote est estimé à 16 km.

[1] Institut de Minéralogie et Pétrographie, Université de Lausanne, BFSH2, CH-1015 Lausanne, Switzerland. <Matthieu.Girard@imp.unil.ch>

Introduction

The Himalayan low temperature metamorphism is poorly known due to the difficulty of finding a suitable method to quantify it. GARZANTI and BRIGNOLY (1989) have studied the Tethyan metasediments in Zanskar. A more precise and restricted study concerns the area between Chumik Marpo and Sarchu in Lahul, where an inverted metamorphism due to thrusting has been proposed (SPRING et al., 1993). This study was extended to the north by STECK et al. (1993). Further south, in the Lesser Himalaya of Garhwal, OLIVER et al. (1995) described diagenetic to epizonal metasediments. In Kumaun JOHNSON and OLIVER (1990) noted anchizonal to epizonal upper Precambrian-lower Paleozoic metasediments. The probable age of this metamorphism is Paleozoic. In the Kathmandu klippe of Nepal an epizonal and higher grade (garnet zone) metamorphism has also been studied with illite crystallinity and b_0 spacing of white mica by MORRISON and OLIVER (1993).

In comparison with the amount of low temperature metasediments that crop out in Himalaya, there are few studies which have characterised the conditions of metamorphism. Our work attempts to improve this situation with an il-

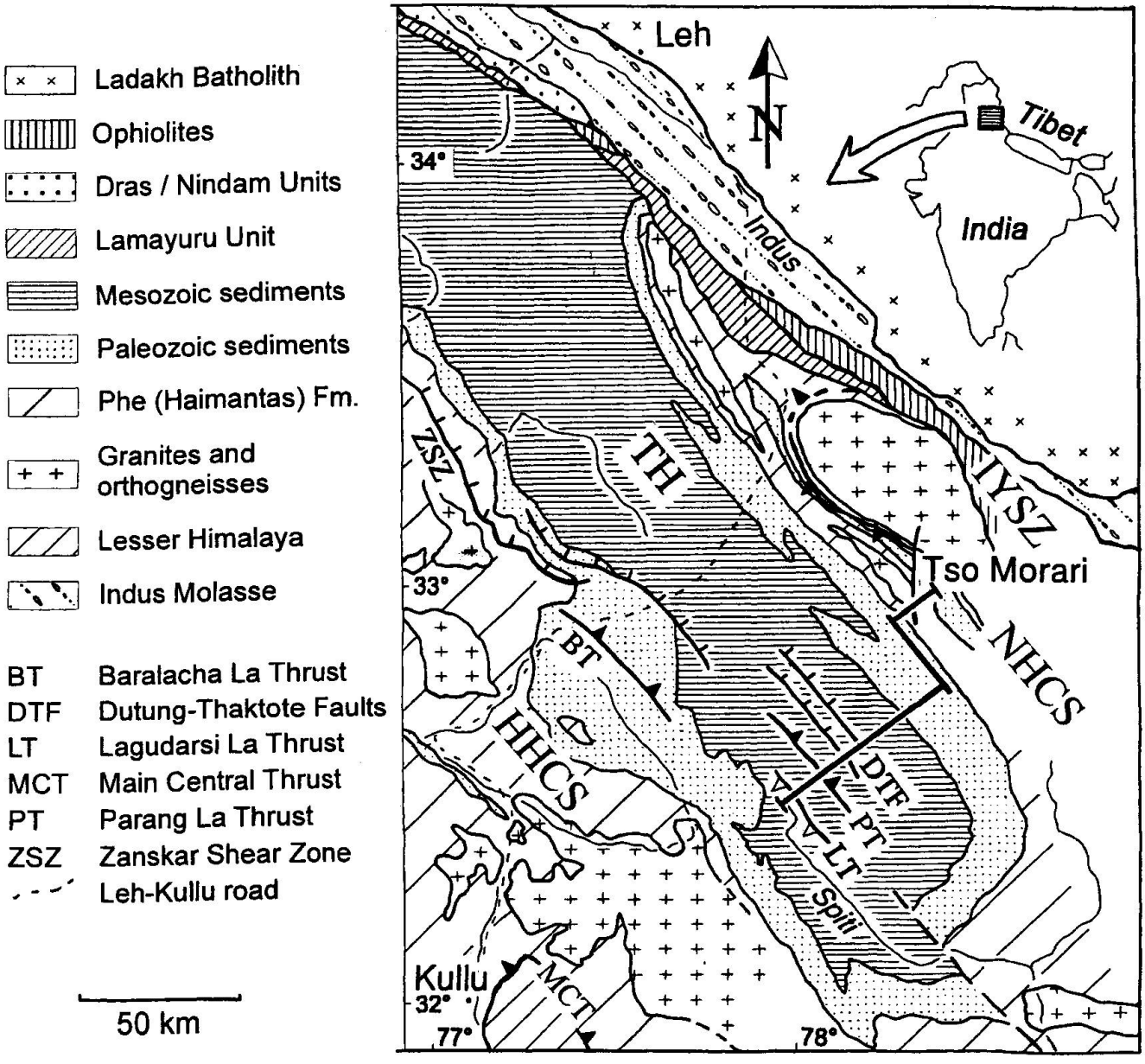

Fig. 1 Geological map showing the location of the studied transect (heavy line) through the Tethyan Zone of NW India. HHCS = High Himalayan Crystalline Sequence; IYSZ = Indus Yarlung Suture Zone; NHCS = North Himalayan Crystalline Sequence; TH = Tethyan Himalaya.

lite crystallinity and clay paragenesis study. For this, marly limestone samples were systematically collected along the Spiti–Tso Morari transect passing by the Parang La and the Takling La (La means pass). This transect is situated in NW India, approximately midway between Leh and Kullu, east of the road joining these two towns (Fig. 1). This area has been described by STECK et al. (1998) who have published and interpreted a new geological map and cross section. The present paper complements this study with low temperature metamorphism data from the southern part of the section. The relationship between the metamorphism and the tectonic features is discussed.

Geological setting

The Himalayan chain is an orogenic mountain belt which can be broadly subdivided in six domains. From south to north we distinguish the Sub-Himalayan molassic hills, the Lesser Himalaya, the High Himalayan Crystalline Sequence (HHCS) which gradually passes to the Tethyan Himalaya (TH). In some areas metamorphic domes forming the North Himalayan Crystalline Sequence (NHCS) crop out between the Tethyan Himalaya and the Indus-Yarlung Suture Zone. The Tso Morari dome, which ends to the north of the section studied, belong to this North Himalayan Crystalline Sequence. The section itself is situated within the sediments of the Tethyan Himalaya.

STRATIGRAPHY

Upper Precambrian to Cretaceous sediments, deposited on the northern passive margin of the Indian plate are exposed in the studied transect. The Precambrian to Cambrian Phe, Karsha and Kurgiakh Formations are composed of an extremely monotonous series of siltstones and impure sandstones. In the Tso Morari area the boundary between the Phe Formation and the two subsequent ones is difficult to distinguish due to the erosion and/or boudinage of the characteristic orange dolomites from the Karsha Formation. Due to the lack of fossils and of marker horizons, it is impossible to say if the Kurgiakh Formation is really present or not. Directly above these metamorphosed siltstones the Permian Kuling Formation occurs. It shows strong lateral variations: in the northern part of the cross section, it consists mainly of crinoids-bearing calcschists, with discontinuous white quartzites and some siltstones; while in the Pradong area (20 km south of the Tso Morari termination) it is represented by fossil bearing sandstones with brachiopods (*Spiriferella*, *Lamnimargus*), conularia and trilobites.

The Triassic Lilang formation shows an increase in the proportion of carbonaceous sediments. It starts with an alternation of decimetric massive limestones containing Upper Smithian ammonites (*Anasibirites* gr. *pluriformis*, *Inyoites*) and marls. Then comes a thick series of marls and subordinate intercalated limestones with *Daonella*. The amount of limestone increases progressively upward in the sequence toward small regularly bedded black micritic limestones that show similarities with the Daonella Limestones from Hanse Formation of Spiti (HAYDEN, 1904). Above these lie massive limestones, sometimes slightly dolomitic or bioclastic, with black Megalodon Limestones. This succession has been attributed to the Early Norian Zozar Formation. The next formation, the Juvavites Beds, forms good stratigraphic marker horizons. These are grey-brown detrital limestones with fine shale intercalations. Some beds are rich in belemnites and brachiopods, and Juvavitidae have been found near Umdung. A massive white coral limestone is sometimes found between the Juvavites Beds and the Monotis Shales, but as this bed is highly discontinuous, distinction between these two formations is often impossible. Above lie the Quartzite Series which are mainly carbonaceous with white and black limestones and dolomites, sometimes siliceous. Real quartzites are rare. The boundary between these Upper Triassic series and the Upper Triassic-Lower Jurassic Kioto limestone is unclear. The Kioto Formation is made of massive white or black limestones, sometimes dolomitic and often bioclastic (small bivalvs, crinoids, corals, gasteropods, Neomegalodon). The black marly Spiti shales of a Malm age, the Lower Cretaceous Giumal sandstones and the white Upper Cretaceous Chikkim limestones and grey marls crop out in an open syncline on the left side of the Spiti river near Chikkim.

The described sedimentary series, starting from the oldest Precambrian to Cambrian rocks found in the north and passing to the Upper Cretaceous Chikkim limestones in the south, shows large stratigraphic gaps when compared with what is described in Spiti (GANSSER, 1964; GARZANTI et al., 1995; HAYDEN, 1904). These gaps only exist in the northern part (Narbu Sumdo area). The principal gap is between the Cambrian Kurgiakh (or even Phe) Formation and the Permian Kuling Formation. Furthermore in the Triassic, due to the low abundance of ammonites, it is difficult to correlate the northern series described

above, with those observed near Lossar in Spiti. However, it is obvious that the facies are different, and as some lithologic members are totally absent in the north (Otoceras bed, Niti Limestone, Nodular Limestone, Grey beds) we suspect that some gaps also exist in the northern Triassic.

TECTONISM AND METAMORPHISM

The studied transect includes in the north the normal limb of the SW verging Mata nappe as defined by STECK et al. (1998), and in the south, the eastern expression of the NE-verging Shikar Beh nappe (EPARD and ESCHER, 1996; STECK et al., 1993; VANNAY and STECK, 1995). South of the Parang and Takling La, SW-verging folds in front and below the Mata nappe have folded the older NE-verging structures of the Shikar Beh nappe (e.g. the Lagudarsi La Thrust). In the eastern transect the Parang La thrust represents the most southern expression of the Mata nappe. This structure also occurs in the western cross section, where it crops out north of the Takling La. However a subsidiary thrust has been observed on the southern side of that pass, suggesting that the Mata nappe extends further south along this transect and that it is not strictly cylindrical. In the frontal part of the Mata nappe, a SW-verging imbricate thrust structure with a first schistosity S1 is observed. In the more internal part of the Mata nappe the structures become more ductile and a second schistosity S2 can be observed in axial surface of large scale SW-verging isoclinal folds (e.g. the Pradong recumbent fold, STECK et al., 1998). As the clay minerals are within these two schistosities, they crystallised either before (detrital origin) or during the SW-verging phase, responsible for the metamorphic peak. An illite with a very small Scherrer width is suspected to be detrital if it coexists with a diagenetic clay mineral paragenesis. The S1 schistosity and thrust surfaces of the Mata nappe are crosscut or reactivated by the NE dipping normal faults of the DTFZ. Similarly, in the more ductile domain further north, the fabrics of S1 and S2 within the Mata nappe are refolded by younger NE-verging backfolds. As the normal faults occur only in the frontal brittle part and the backfolds only in the more internal ductile part of the Mata nappe, with no interaction of the two, we interpret these tectonic features as belonging to the same tectonic event, but acting at different tectonic levels.

The Dutung-Thaktote normal fault zone is an example of synorogenic extension in the Central Himalaya. This forms the eastern equivalent to the ductile Zanskar Shear Zone (HERREN, 1987), which was active between about 23 Ma and 19.8 Ma (DÈZES et al., 1999). But as the DTFZ crops out in a higher tectonic level, it represents the brittle domain, and is suspected to pass to the ductile regime at deeper levels. These Himalayan extensional structures are referred to as the North Himalayan Shear Zone (PÊCHER, 1991) or the South Tibetan Detachment System (STDS after BURCHFIELD et al., 1992). As these extensional structures are situated in the middle of the Himalayan chain between the Indus Suture to the N and the Main Boundary Thrust to the S, we suggest a new name, the *Central Himalayan Detachment System.*

The mineral paragenesis observed in the field indicate that in the Mata nappe the metamorphism decreases from north to south. Staurolite-kyanite-sillimanite assemblages occur in the Tso Morari Dome near Nuruchan. The southern limit of the garnet zone is situated above the Ordovician Rupshu granite. Further south we find chloritoid and finally biotite disappears at Narbu Sumdo (STECK et al., 1998). As no index minerals can be directly observed south of this point, the metamorphic gradients that exist between Narbu Sumdo and the Spiti river could not be determined from field observations. Therefore these rocks were investigated for their clay mineralogy.

Sampling and analytical procedure

Samples were taken from the Tso Morari to the N, along the Parang Valley, across the Parang and Takling La, through the Takling Valley down to Spiti valley near Kiato and Chikkim. Younger and younger stratigraphic formations outcrop from north to south. Brief sample descriptions are given in table 1.

One sample comes from the Cambrian Phe Formation. It is a micaceous sandstone that has been transformed into a quartzschist. The Permian samples are greywackes and crinoids-bearing calcschists. In the Triassic Formations, black micritic limestones from the Daonella Limestones have been sampled along with one white coral limestone from the Nimaloksa Formation, intercalated in the Daonella Limestones. Samples from Zozar Formation are black micritic limestones. One sample comes from a white coral limestone boudin between the Juvavites Beds and the Monotis Shales, and a grey siliceous limestone comes from the Juvavites Beds. In the Quartzite Series, white and black micritic limestones were sampled. They usually contain only minor amounts of quartz or are devoid of this mineral altogether. Samples from the Kioto Formation are

Tab. 1 Description of the studied samples collected along the Spiti river–Tso Morari transect listed from SW to NE. FWHM values in brackets refer to the samples where a detrital component may be present. AS 121 and AS 122 are chloritoid bearing samples, not analysed for illite crystallinity. Juv. = Juvavites; L = limestone; P = Permian; PC-C = Precambrian-Cambrian; UC = Upper Cretaceous; UTr = Upper Triassic.

Samples		Lithology	Formation	Tectonic unit	FWHM $\Delta 2\theta°$ CuKα
AS	161	micritic L.	Chikkim L., UC	East Shikar Beh	
AS	162	micritic L.	Chikkim L., UC	East Shikar Beh	
AS	168	grey marble	Kioto, Liassic	East Shikar Beh	0.51
AS	169	grey L.	Kioto, Liassic	autochthonous	(0.14)
G	1	black micritic L.	Zozar, UTr	autochthonous	0.26
G	2	black micritic L.	Zozar, Tr	autochthonous	0.20
AS	32	grey micritic L.	Qzite series, Tr	autochthonous	(0.11)
AS	33	black micritic L.	Qzite series, Tr	autochthonous	0.20
G	3	white marble	Qzite series, Tr	autochthonous	(0.09)
G	4	black micritic L.	Qzite series, Tr	autochthonous	0.17
G	5	grey L.	Kioto, Liassic	Mata Nappe	(0.12)
G	6	grey L.	Kioto, Liassic	Mata Nappe	(0.09)
G	8	black mylonitic L.	thrust	Takling La Thrust	(0.11)
G	10	grey marble	thrust	Takling La Thrust	(0.18)
G	11	white marble	Qzite series, UTr	Mata Nappe	(0.10)
G	12	black micritic L.	Kioto, Liassic	Mata Nappe	0.21
AS	153	grey L.	Qzite series, UTr	Mata Nappe	(0.10)
G	7	bioclastic nodulous L.	Qzite series, UTr	Mata Nappe	(0.13)
AS	35	grey micr. L.	Qzite series, UTr	Mata Nappe	0.39
G	13	grey siliceous L.	Juv. beds, UTr	Mata Nappe	0.65
G	14	grey L.	Coral L., UTr	Mata Nappe	0.96
G	16	black micritic L.	Hanse, UTr	Mata Nappe	1.2
AS	146	black micritic L.	Hanse, UTr	Mata Nappe	1.53
G	17	black micritic L..	Hanse, UTr	Mata Nappe	1.42
AS	140	black micritic L.	Hanse, UTr	Mata Nappe	0.45
G	18	white coral L.	Nimaloksa, UTr	Mata Nappe	0.27
G	22	black micritic L.	Hanse, UTr	Mata Nappe	0.28
G	32	black micritic L.	Hanse, UTr	Mata Nappe	
AS	38	siliceous calcschist	Kuling, P	Mata Nappe	0.24
AS	40	siliceous calcarenite	Juv. beds, UTr	Mata Nappe	(0.21)
G	35	greywack	Kuling, P	Mata Nappe	0.19
G	37	siliceous calcschist	Kuling, P	Mata Nappe	
G	39	greywack	Kuling, P	Mata Nappe	0.17
G	40	quartzschist	Phe, PC-C	Mata Nappe	0.22
AS	121	siliceous calcschist	Kuling, P	Mata Nappe	
AS	122	siliceous calcschist	Kuling, P	Mata Nappe	

grey clear limestones very poor in clay minerals, or black micritic limestones. The Upper Cretaceous Chikkim limestone is a micritic foraminiferal limestone poor in clay minerals.

500 g to 1 kg of each sample were crushed to a size of 1–2 mm. Insoluble minerals were separated from carbonates by dissolution in 2M HCl and agitating for 20 minutes, and then neutralised to pH 5.6 with distilled water. Grain size separation (< 2 μm) was achieved by centrifugation at pH 7.5 (MOORE and REYNOLDS, 1989). The < 2 μm size fraction was saturated with Ca^{2+} using 1M $CaCl_2$, the solution being changed once during the 36 hours period, and the clays were then washed until they not longer flocculated.

Approximately 2.5 ml of suspension were sedimented on a glass slide. To measure illite crystallinity, we used only the slides with more than 2.5 mg/cm^2 of material, following the recommendations suggested by FREY (1988) and our own experiments (JABOYEDOFF and THÉLIN, 1996) which confirm that very thin preparations lead to a decrease in illite crystallinity (i.e., the Scherrer width).

XRD data were collected with a Rigaku automated diffraction system, using a Rotaflex generator with a rotating Cu anode at 40 kV and 30 mA conditions, an horizontal Geigerflex goniometer (200 mm radius), a nickel filter, 0.5° divergence and scatter slits, 0.15 mm receiving slit and 5°

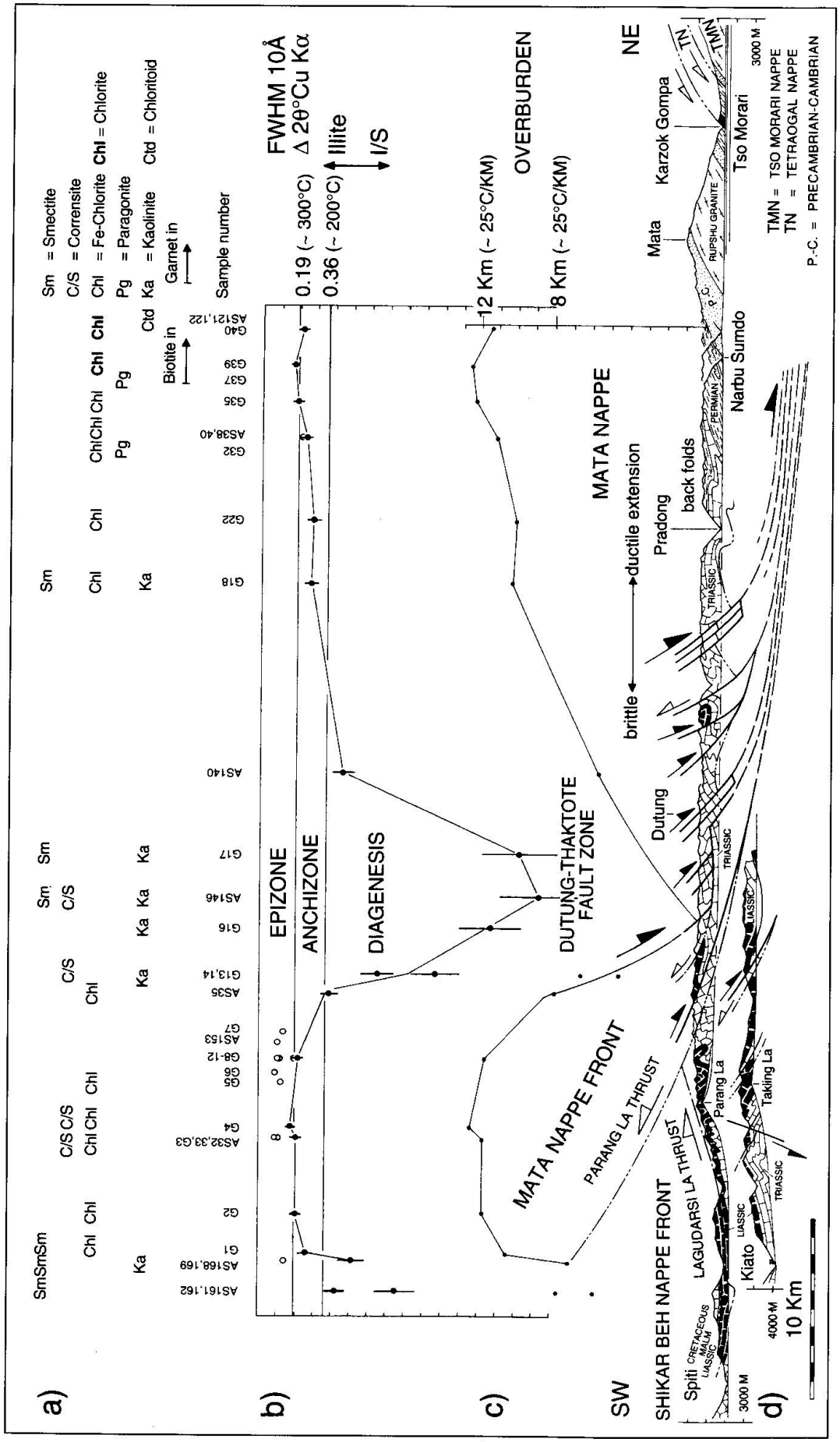

Fig. 2 The Spiti river–Tso Morari transect showing (a) Clay size paragenesis and index minerals in the studied samples. Minerals in brackets are not in equilibrium with the measured illite. (b) Illite crystallinity (FWHM) in terms of Scherrer width at half-peak height (001 reflection of illite on glycolated samples < 2 μm), vertical bars represent a 14% error as proposed by Robinson et al. (1991). (c) The estimated overburden is deduced from the FWHM data, according to the FWHM-temperature relation of figure 4 and a geothermal gradient of 25 °C/km. (d) Geology along the two transects. The Takling La transect is situated W of the Parang La transect and joints with the second transect at Dutung.

Soller slits. For characterising clay phases, we used continuous scans (2° 2θ/min scan speed, step sampling 0.02° 2θ) and for the illite crystallinity method (Scherrer width measurement), we used step scanning (0.01° 2θ steps and a counting time of 2" per step). The preparations were first run in the air-dried state and then again after 24 hrs saturation with ethylene glycol vapour and then finally heated to 550 °C for 1 hr. The Scherrer width was measured from XRD patterns of air-dry samples (FREY, 1987; KÜBLER, 1967). This latter measurements were performed using the software "QUICK WIDTH" (© JABOYEDOFF, 1997) without any smoothing or Kα2 stripping; by this way we consider the full width half-maximum (FWHM), as indicated in figure 2 and table 1. Based on the University of Lausanne Rigaku XRD system, the Scherrer width limits used in this study are 0.19° Δ2θ° (CuKα) for the epizone-anchizone boundary and 0.36° Δ2θ° (CuKα) for the anchizone-deep diagenesis boundary. For a Δ2θ° (CuKα) > 0.50°, we consider that illite is no longer pure and the dominant phase is an illite/smectite mixed layer mineral (I/S), with a low smectitic content, as discussed by JABOYEDOFF and THÉLIN (1996). The mentioned limits were calibrated using standard from KÜBLER (1968). JABOYEDOFF et al. (submitted) have used data from the Swiss Alps to compare statistically our results with other scales like the crystallinity index standard scale (WARR and RICE, 1994).

As different FWHM were obtained in samples of the same lithology (i.e. black micritic limestones) we can rule out a lithological control on the FWHM results.

As the present study is regional, we intentionally did not consider crystallo-chemical complexities related to the FWHM of the 001 peak of illite, such as small smectite content leading to mixed-layering, size of coherent diffraction domain and lattice distorsion. More details of these influences can be found in KÜBLER (1990), LANSON and CHAMPION (1991), POLLASTRO et al. (1995), and JABOYEDOFF et al. (in press). That the FWHM of anchizonal and epizonal illite is not strongly influenced by mixed layer smectite was confirmed by missing deviation after glycolation as far as 2θ° (CuKα) (001) is considered, by an intensity ratio of around 1 as defined after SRODON and EBERL (1984), and a Δ2θ° value > 8.7, defined as 2θ° (002I/003S) – 2θ° (001I/002S) by MOORE and REYNOLDS (1989). Smectite content therefore forms only 2–3% of the I/S mixed-layer mineral, assuming a Reichweite = 0.

Results

Illite crystallinity

The sixty km long transect, from SW (Spiti river) towards NE (Tso Morari), shows strong differences in the FWHM measurements on illite. There are three contrasting domains (Fig. 2):

1) A SW domain begins with increasing Δ2θ° values between middle diagenetic grade in the Chikkim limestones (I/S mixed-layer phases) and upper anchizonal (illite) conditions, at the mouth of the Takling river. From samples G1 to G12 the FWHM trend forms a plateau indicating upper anchizonal to low epizonal conditions with an average of around 0.20 Δ2θ°. In figure 2 the unfilled circles represents doubtful values: the 0.10 Δ2θ° average values indicate a very high degree of order, especially for a powder, which might be interpreted as due to detrital inheritance. However, the lack of other less ordered illitic phases in these samples suggests that these sharp reflections do indeed represent metamorphic illite-muscovite of epizonal grade metamorphism. In any case, the full circle values clearly reveal epizonal conditions.

2) A central domain shows a significant decrease in metamorphic grade with FWHM values indicating diagenetic conditions. The sharp decrease in grade, spanning the anchizone-diagenesis boundary until diagenetic conditions is highlighted by an I/S mixed-layer phase with a 10 Å peak broader than 1.4 Δ2θ°. The NE side of the curve shows Δ2θ° values drastically decreasing down to 0.45°, i.e. upper diagenetic conditions.

3) A NE domain with a continuous increase of metamorphism towards the NE ranges from upper diagenetic conditions, through whole anchizone, up to low epizonal conditions. The Δ2θ° values range from 0.45° to 0.17°. The narrowing of the illite 10 Å peak, accompanied by the disappearance of smectite, is well illustrated on figure 3. Samples from the northern end of the profile contain chlorite (001 peak survives 550 °C heating), paragonite, biotite and chloritoid, indicating that greenschist conditions were reached. Further north, the appearance of garnet, hornblende and finally of the assemblage sillimanite + kyanite + staurolite indicate that the metamorphic grade continues to increase (STECK et al., 1998).

Other clay phases

In addition to the properties of illite, other clay phases also indicate low temperature metamorphic conditions. Kaolinite, with an 001 peak at 7.16 Å, appears quite ubiquitous within diagenetic and middle anchizonal micritic limestones, especially in the central domain (DTFZ). A regular

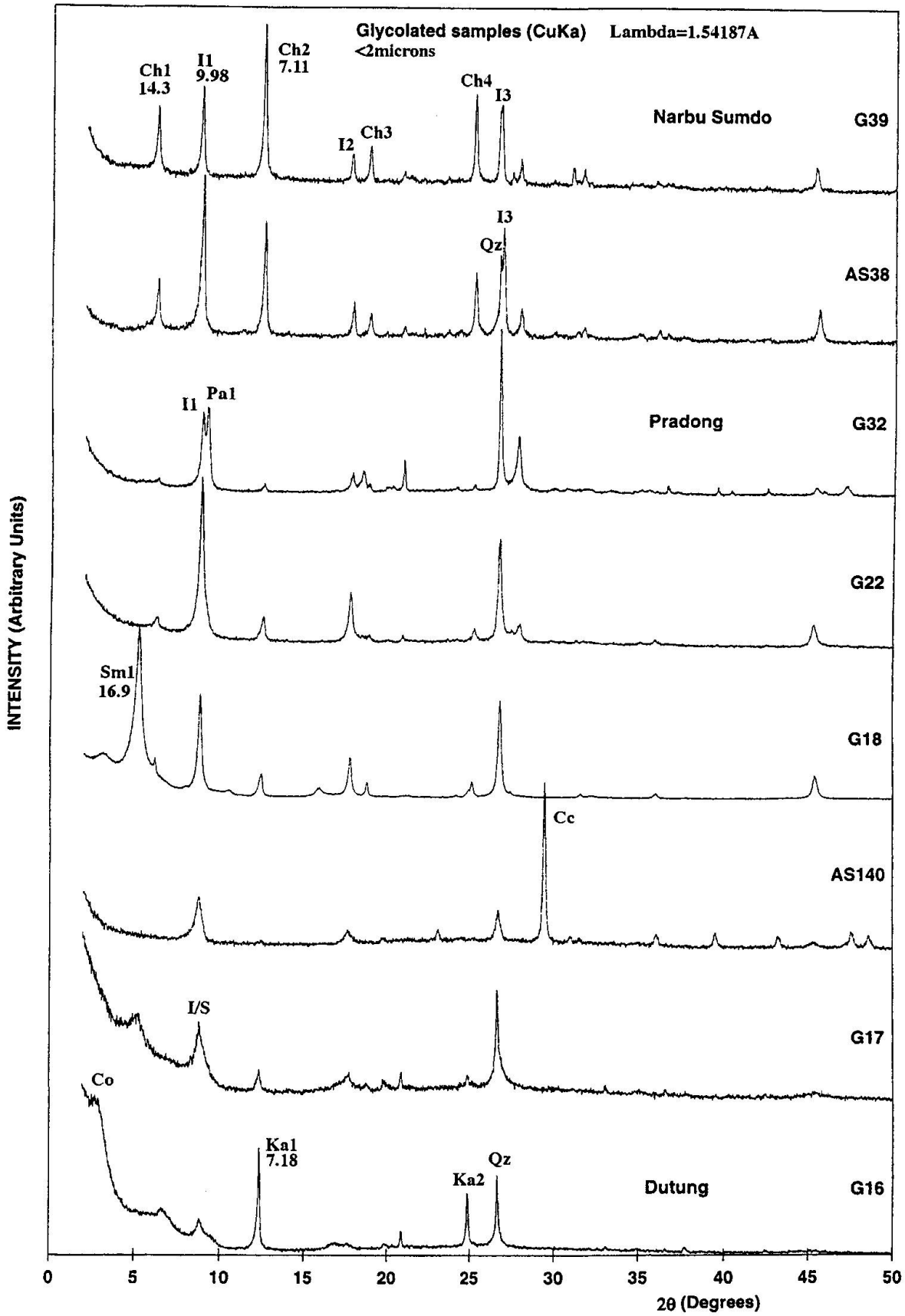

Fig. 3 XRD patterns of glycolated samples (< 2 μm). Samples G16 to G39 are arranged from SW to NE (see Fig. 2 for a more precise location). Cc = calcite; Chl = chlorite; Co = corrensite; I = illite; I/S = illite/smectite mixed-layered clay mineral; Ka = kaolinite (presence confirmed by hydrazine test); Pa = paragonite; Sm = smectite. 1,2,3,4 indicate the order of the 00l reflection.

mixed-layer phase detected by a superstructure peak at 31–32 Å and rational harmonics, is considered to be corrensite (ordered interstratified chlorite/smectite). Its occurrence appears to be more controlled by lithologically related factors, such as rock chemistry than by metamorphic conditions, as it is recorded preferentially in black micritic limestones. It seems to be stable from middle diagenetic conditions till the anchizone-epizone boundary. Discrete grains of smectite are present only within very low grade metamorphic samples, except in sample G18 which is assigned to middle anchizonal conditions. In this sample, smectite (mostly dioctahedral with 2-H_2O layers) coexists with neoformed illite or I/S and therefore, it is possible to consider this smectite as a late retrogression phase. In several samples, there is an interesting 14.15 to 14.20 Å phase, which did not solvate after glycolation and which is considered to be iron-rich chlorite (BRINDLEY and BROWN, 1980; MOORE and REYNOLDS, 1989). This chlorite 001 peak does not usually survive after heating to 550 °C, except in samples from the extreme NE of the studied profile, which are of greenschist facies (biotite zone).

Discussion of a tectonic model

According to several studies of fluid inclusions and oxygen isotopic temperatures, the onset of the anchizone is at ca. 230 °C and its upper limit is between 300 and 350° (FREY, 1987; FREY and ROBINSON, 1999). In this study the temperatures of 200 °C and 300 °C have been admitted as corresponding to the lower and upper limits of the anchizone, as proposed by JABOYEDOFF and THÉLIN (1996) (Fig. 4). However, we are perfectly aware that the illite crystallinity method is not a quantitative thermometer. The temperature estimates must be considered as an order of magnitude, namely because stress, kinetic factors, bulk chemistry and inherited mineralogy influence also the "illitic system".

Along the Spiti–Tso Morari transect, the illite crystallinity results indicate that the grade of metamorphism reaches the anchizone-epizone limit at two places. The overburden can be estimated if the thermal gradient is known. Preliminary results of thermobarometry on garnet and kyanite bearing metapelites from the area indicate a thermal gradient of about 25 °C/km, in agreement with the measurements of EPARD et al. (1995) and DÈZES et al. (1999) in the High Himalayan Crystalline Sequence of the Kullu Valley and Zanskar, respectively. On the basis of this geothermal gradient the minimal overburden has been estimated and is presented in figure 2c. The overburden curve becomes less precise when the $\Delta 2\theta°$ values increase. According to the variability proposed by JABOYEDOFF and THÉLIN (1996)

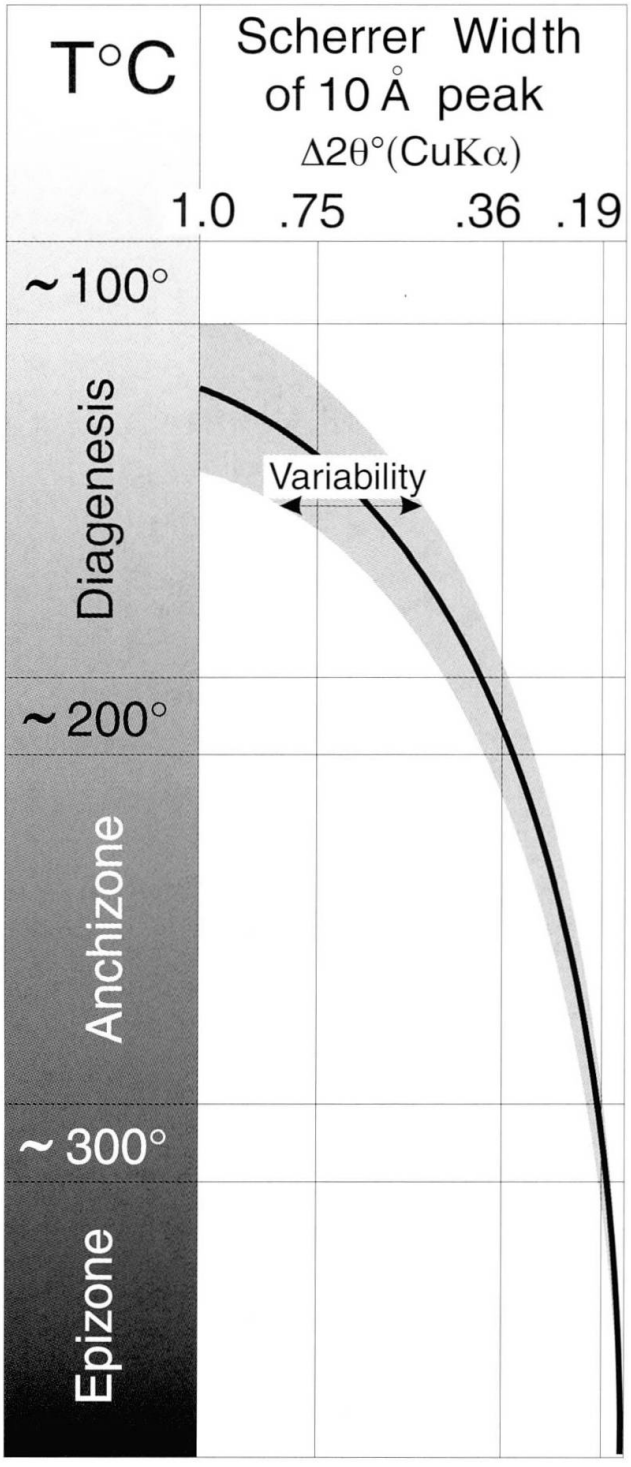

Fig. 4 FWHM (or Scherrer width)-temperature relation curve. The 0.19° and 0.36° $\Delta 2\theta°$ (CuKα) are the upper and lower anchizonal boundary limits of the X-ray laboratory (Rigaku diffractometer) of the Inst. Mineral. and Petro., Univ. Lausanne. Modified after JABOYEDOFF and THÉLIN (1996) and references therein.

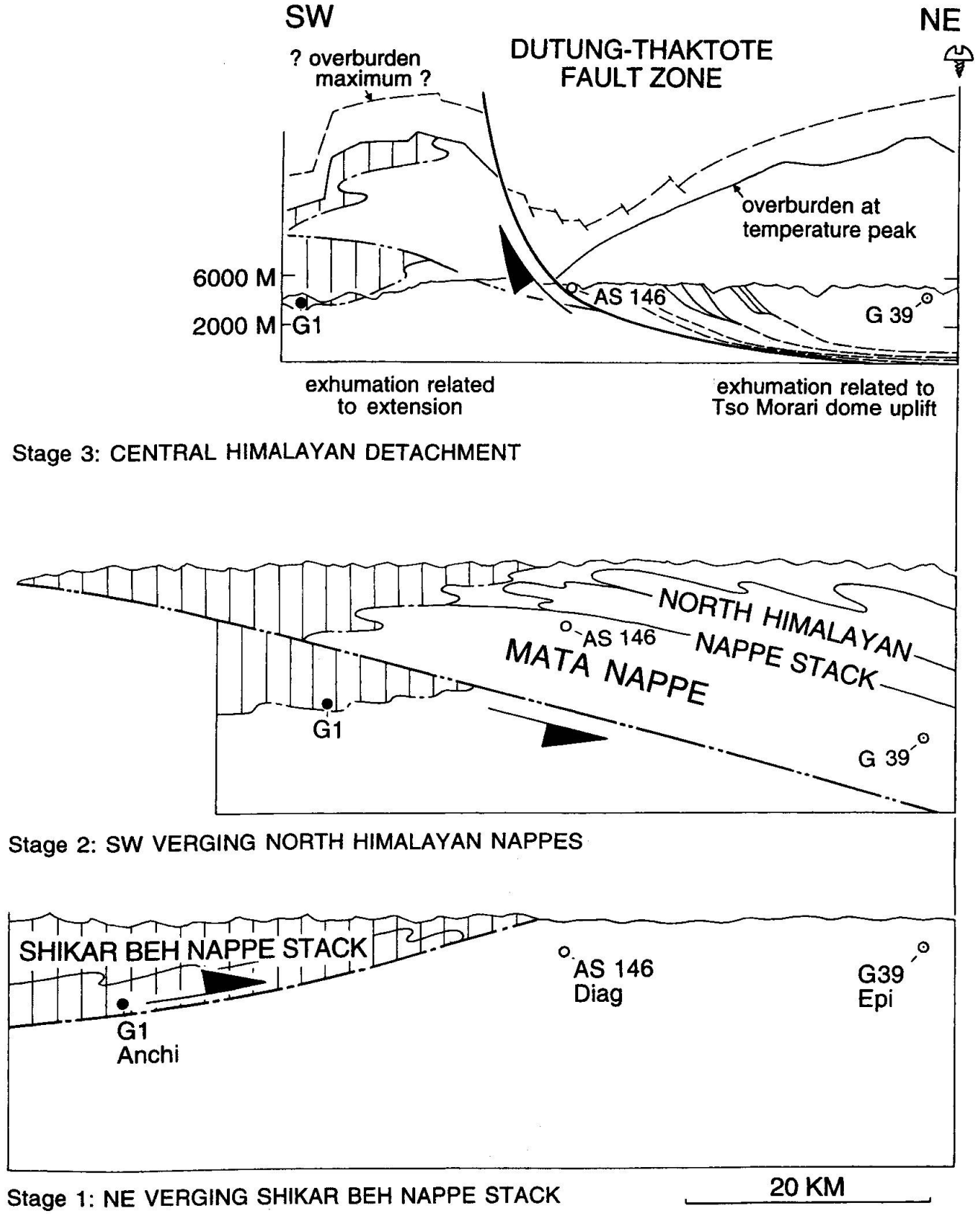

Fig. 5 Schematic interpretation of the exhumation of the anchizonal-epizonal rocks from the Spiti river–Tso Morari cross section. Three samples (G1, AS146, G39) are shown on the cross section which are representative of the different metamorphic zones. Stages 1 to 3 illustrate the three main tectonic events: (1) the thrusting of the Shikar Beh nappe toward the NE, (2) SW directed emplacement of the North Himalayan nappes and (3) extension along the Dutung-Thaktote fault zone, accompanied by differential uplift and erosion. The latter event could be synchronous to the ca. 20 Ma Zanskar Shear Zone (DÈZES et al., 1999).

(Fig. 4), an illite crystallinity of 0.75° Δ2θ° gives an approximate uncertainty of ± 0.6 km, and the FWHM-temperature correlation can not be established for Δ2θ° values greater than 1.0°. For this reason the overburden curve is not constrained for samples AS146, G16 and G17 (Fig. 2). Nevertheless the ~ 300 °C inferred from the illite crystallinity data at Narbu Sumdo, and at the area of the passes, imply an overburden of 12 km. However, as this overburden is dependent of the FWHM-temperature relationship and of the thermal gradient which are both not well constrained, this overburden of 12 km is only an approximation. Nevertheless the relative differences between the samples are independent of these two assumptions and are coherent with the previously observed tectonic structures (STECK et al., 1998).

As all samples except G40 are of Permian or younger age, the initial sedimentary cover did not exceed 4 km in thickness. This is three time less than that considered necessary to account for the observed metamorphism. To explain this metamorphism we propose a nappe tectonic model based on the structures previously observed on the field. There is no metamorphic jump across the thrusts of the Mata and Shikar Beh nappes. It is therefore clear that the observed low temperature metamorphism has been generated synchronous with the emplacement of the two nappes. If the thickness of the Mata nappe logically decreases towards its frontal part, it is paradoxical that the metamorphism is identical in Narbu Sumdo (NE area) and near the passes (SW area). To explain this we suggest that the overburden was made up of the superposition of two nappes in the SW area. The structures observed in the field and described in the introduction imply that it is the younger Mata nappe which extents further south over the Shikar Beh nappe, rather than the opposite relationship. The metamorphic decrease recorded in the last four samples in the SW probably corresponds to the frontal part of the Mata nappe.

The minimum overburden curve presented in Fig. 2c is not considered to represent a paleotopography, but may simply reflect the overburden differences along the profile during peak metamorphism. Due to erosion, it is probable that the topography never exceeded more than the present altitude of 6000 m. After the nappe emplacement, which ended at about 30 Ma (Ar/Ar age on micas, DE SIGOYER et al., 1997), the anchizonal-epizonal rocks were exhumed to the surface by two different tectonic processes. In the SW area, a strong isostasic uplift is probably due to the overlying denudation along the DTFZ. These post-metamorphic normal faults have exhumed the rocks from a depth of about 12 km and displaced them against the diagenetic rocks from Dutung, which did not change their tectonic position during this time (Fig. 5). In addition to the observed normal faults we propose a major extensional fault with an offset of about 13 km at the river confluence at Dutung. This fault is responsible for the thick alluvial deposits which hide it. Adding together the total measured offset of the other mapped extensional faults (~ 3.5 km), a total offset of about 16 km is estimated. This probably represents a minimum value considering that isostatic movements and erosion were active during the extension. In the NE area the 12 km of exhumation proposed for the low epizonal rocks cannot be explained by the same process, as no normal faults have been observed. In this area exhumation was due mostly to backfolding and to the formation of the Tso Morari dome which gave rise to significant erosion and isostatic compensation.

Conclusions

Structural work, combined with the study of the metamorphic clay mineral assemblages by X-ray diffraction methods, have been applied to estimate the tectonic overburden in the Tso Morari–Spiti transect during the emplacement of the Mata and Shikar Beh nappes. The middle of the cross section is characterised by diagenetic grade and is bordered by two zones of anchizonal to epizonal grade. Field observations indicate that this metamorphic decrease is caused by the Dutung-Thaktote extensional fault zone. This fault zone overprints older structures of the Mata nappe. Furthermore, these data have been used to reconstruct the amount of offset along this fault zone. It is suggested that the DTFZ, with its minimum offset of 16 km, represents a major extensional structure of the Central Himalayan detachment system [= North Himalayan Shear Zone, (PÊCHER, 1991); South Tibetan detachment system (BURCHFIELD et al., 1992)].

Acknowledgements:

Financial support for this work was provided by the Swiss National Fund for scientific research (grants n° 20-45063.95/1 and 20-52165.7) within the context of the Ph.D. thesis of the first author. L. Dufresne and O. Lokosha are kindly thanked for preparing samples and performing the XRD analyses. Journal reviewers L.N. Warr and G.J. Oliver are thanked for their constructive remarks.

References

BRINDLEY, G. and BROWN, G. (1980): Crystal structures of clay minerals and their X-ray identification. Mineralogical Society, London, 495 pp.

BURCHFIELD, B.C., CHEN, Z., HODGES, K.V., LIU, Y., ROYDEN, L.H. and DENG, C. (1992): The South Tibetan Detachment System, Himalayan orogen: extension contemporaneous with and parallel to shortening in a collisional mountain belt. Geol. Soc. Amer. Spec. Paper 269, 41 pp.

DE SIGOYER, J., GUILLOT, S., LARDEAUX, J.M. and MASCLES, G. (1997): Glaucophane bearing eclogites in the Tso Morari dome (Eastern Ladakh, NW Himalaya). Eur. J. Mineral., 9, 1073–1083.

DÈZES, P., VANNAY, J.C., STECK, A., BUSSY, F. and COSCA, M. (1999): Synorogenic extension: Quantitative constraints on the age and displacement of the Zanskar Shear Zone (NW Himalaya). Geol. Soc. Amer. Bull., 111, 364–374.

EPARD, J.L. and ESCHER, A. (1996): Transition from basement to cover: a geometric model. J. Structural Geol., 18, 533–548.

EPARD, J.L., STECK, A., VANNAY, J.C. and HUNZIKER, J. (1995): Tertiary Himalayan structures and metamorphism in the Kulu Valley (Mandi-Khoksar transect of the Western Himalaya) Shikar Beh Nappe and Crystalline Nappe. Schweiz. Mineral. Petrogr. Mitt., 75, 59–84.

FREY, M. (1987): Low temperature metamorphism. Blackie and Son, Glasgow and London, 351 pp.

FREY, M. (1988): Discontinuous inverse metamorphic zonation, Glarus Alps, Switzerland: evidence from illite "crystallinity" data. Schweiz. Mineral. Petrogr. Mitt., 68, 171–183.

FREY, M. and ROBINSON, D. (1999): Low-Grade Metamorphism. Blackwell Science, Oxford, 313 pp.

GANSSER, A. (1964): Geology of the Himalayas. John Wiley & Sons, London, 289 pp.

GARZANTI, E. and BRIGNOLI, G. (1989): Low temperature metamorphism in the Zanskar sedimentary nappes (NW Himalaya, India). Eclogae geol. Helv., 82(2), 669–684.

GARZANTI, E., JADOUL, F., NICORA, A. and BERRA, F. (1995): Triassic of Spiti (Tethys Himalaya, N-India). Rivista Italiana di Paleontologia e Stratigrafia, 101/3, 267–300.

HAYDEN, H.H. (1904): Geology of Rupshu. Geological Survey of India, 36/1, 92–100.

HERREN, E. (1987): Zanskar shear zone; northeast-southwest extension within the Higher Himalayas (Ladakh, India). Geology, 15, 409–413.

JABOYEDOFF, M., ADATTE, T., GOY-EGGENBERGER, D., KÜBLER, B., MAIGNAN, M. and THÉLIN, P. (submitted): Inter Laboratory "Illite Crystallinity" calibration: theoretical and practical approach. Eur. J. Mineral.

JABOYEDOFF, M., KÜBLER, B. and THÉLIN, P. (in press): Illite crystallinity revisited. Clays and Clay minerals.

JABOYEDOFF, M. and THÉLIN, P. (1996): New data on low-grade metamorphism in the Briançonnais domain of the Prealps, Western Switzerland. Eur. J. Mineral., 8, 577–592.

JOHNSON, M.R.W. and OLIVER, G.J.H. (1990): Precollision and postcollision thermal events in the Himalaya. Geology, 18, 753–756.

KÜBLER, B. (1967): La cristallinité de l'illite et les zones tout à fait supérieur du métamorphisme. Colloque de Neuchâtel, 1966, p. 105–121. La Baconnière, Neuchâtel.

KÜBLER, B. (1968): Evaluation quantitative du métamorphisme par cristallinité de l'illite. Bull. Centre. Rech. Pau SNPA, 2, 385–397.

KÜBLER, B. (1990): "Cristallinité" de l'illite et mixed-layers: brève révision. Schweiz. Mineral. Petrogr. Mitt., 70, 89–93.

LANSON, B. and CHAMPION, D. (1991): The I/S-to-illite reaction in the late stage diagenesis. Amer. J. Sci., 291, 473–506.

MOORE, D.M. and REYNOLDS, R.C.J. (1989): X-ray diffraction and the identification and analysis of clay minerals. Oxford University Press, Oxford and New York, 331 pp.

MORRISON, C.W. and OLIVER, G.J.H. (1993): A study of illite crystallinity and fluid inclusions in the Kathmandu Klippe and the Main Central Thrust zone, Nepal. Geol. Soc. Spec. Publ., 74, 525–540.

OLIVER, G.J., JOHNSON, M.R.W. and FALLICK, A.E. (1995): Age of metamorphism in the Lesser Himalaya and the Main Central Thrust Zone, Garhwal India; results of illite crystallinity, ^{40}Ar-super ^{39}Ar fusion and K–Ar studies. Geol. Magazine, 132, 139–149.

PÊCHER, A. (1991): The contact between the HHC and the Tibetan sedimentary series: Miocen large-scale dextral shearing. Tectonics, 10/3, 587–598.

POLLASTRO, R.M., MCLEAN, H. and ZINK, L.L. (1995): Reconnaissance bulk-rock and clay mineralogies of argillaceous Great Valley and Franciscan strata, Santa Maria Basin Province, California. In: USGS Bull.: Conglomerates of the upper middle Eocene to lower Miocene Sespe Formation along the Santa Ynez Fault; implications for the geologic history of the eastern Santa Maria Basin area, California. 11–113.

SPRING, L., MASSON, H., STUTZ, E., THÉLIN, P., MARCHANT, R. and STECK, A. (1993): Inverse metamorphic zonation in very low-grade Tibetan zone series of Zanskar and its tectonic consequences (NW India, Himalaya). Schweiz. Mineral. Petrogr. Mitt., 73, 85–95.

SRODON, J. and EBERL, D.D. (1984): Illite. In: BAILEY, S.W. (ed.): Reviews in mineralogy. Micas, p. 495–544. Mineralogical Society of America.

STECK, A., EPARD, J.L., VANNAY, J.C., HUNZIKER, J., GIRARD, M., MORARD, A. and ROBYR, M. (1998): Geological transect across the Tso Morari and Spiti areas: The nappe structures of the Tethys Himalaya. Eclogae geol. Helv., 91, 103–121.

STECK, A., SPRING, L., VANNAY, J.C., MASSON, H., STUTZ, E., BUCHER, H., MARCHANT, R. and TIÈCHE, J.C. (1993): Geological transect across the northwestern Himalaya in eastern Ladakh and Lahul (a model for the continental collision of India and Asia). Eclogae geol. Helv., 86, 219–263.

VANNAY, J.C. and STECK, A. (1995): Tectonic evolution of the High Himalaya in Upper Lahul (NW Himalaya, India). Tectonics, 14, 253–263.

WARR, L.N. and RICE, A.H.N. (1994): Interlaboratory standardization and calibration of clay mineral crystallinity and crystallite size data. J. Metam. Geol., 12, 141–152.

Manuscript received October 15, 1998; revision accepted June 16, 1999.